Poynting singularities in optical dynamic systems

A. V. Novitsky* and L. M. Barkovsky
Department of Theoretical Physics, Belarusian State University, Nezavisimosti Avenue 4, 220030 Minsk, Belarus
(Received 15 January 2009; published 16 March 2009)

We develop the theory of the Poynting singularities (critical points of the Poynting vector) extending the theory of dynamic systems to classify and analyze optical singularities. An optical dynamic system is described by the three first-order differential equations for the image point, with the tangent to the image point trajectory being the Poynting vector. Important feature of the Poynting singularities is the existence of the polarization-induced singularities (arise due to the specific field polarization) along with the field-induced ones (appear owing to the vanishing the fields). We analyze not only isolated critical points, but the manifolds of singularities forming lines and surfaces as well. We define the types of the singular points (vortex, saddle, sink, source, and focus) using the trace and determinant of the stability matrix. Such a criterion and the study of the dependence on parameter (bifurcations) are applied for a number of examples. We offer to study the chaotic dynamic of the image point in future.

DOI: 10.1103/PhysRevA.79.033821 PACS number(s): 42.25.−p, 05.45.−a, 41.20.Jb, 42.90.+m

I. INTRODUCTION

Singular optics deals with complex field distributions. The complexity is connected not only with intricate intensity patterns, but with inhomogeneous spatial pictures of elliptical polarization. The fields can be decomposed into the plane waves (or any other orthogonal waves) and can be computed using the Fourier-transform technique. Singularities are the result of the complex behavior of the fields, in other words, result of the wave interference. The reason why we study singularities is not only fundamental (to deeply understand the peculiarities of the inhomogeneous field distributions). The point is that the complex field distributions are generated in laser devices, while the fields themselves are applied in super-resolution lenses [1–8]. Focusing beyond the diffraction limit is caused by the evanescent waves. The lenses (and their singularities) are intensively discussed now [9,10].

Electromagnetic beams have been studied for a long time in wave or ray formulation (e.g., see [11]). Sometimes the scalar approximation is useful. In general, when polarization plays important part, the *vector* beams must be considered. The beams can be described just by the electric and magnetic field strengths. One more description is the use of the beam tensor introduced in [12,13]. This tensor entirely describes the light beam (including partially polarized beams) and can be applied to find the result of the reflection, refraction, scattering, and so on.

The history of the problem may make clear some details and help to grasp the classes of singularities. The story starts with the classical paper of Nye and Berry [14], who described the creation of the wave crests in the ultrasonic field. These crests were called edge dislocations of the wave front by analogy with dislocations in crystals. It was discovered that at the dislocation point the wave amplitude turns to zero; hence, the wave phase is not defined. This property corresponds to the wave singularity (exactly, *phase singularity*). Later on, the singularities have been developed in many investigations.

*andrey.novitsky@tut.by

The ultrasonic field is a scalar one; therefore, the theory of singularities cannot be directly applied to vector electromagnetic fields. Nevertheless a linearly polarized field can be considered as scalar field. The zeroes of the vector field can be also considered as phase singularity (the phase is not defined). On the other hand, the vector nature implies that at the point of zero vector magnitude its direction is not defined as well. In paper [15] such a singularity is called a vector one. Further the *polarization singularity* was introduced [16–21]. It arises in an inhomogeneous distribution of elliptically polarized field, which is considered as generic. Each point of this field may have not only distinct wave amplitudes and phases, but wave polarizations (azimuths and ellipticities of the polarization ellipses) too. Polarization singularities include C point (points of circular polarization, at which the polarization azimuth is not defined) and L points (points of linear polarization, at which the right- or left-handed direction of the elliptical polarization is not defined). The amplitude does not vanish at the polarization-singular points and, therefore, the phase and the vector direction are defined. Vector and polarization singularities lead to the polarization [15] and vortex [22] flowers, optical diabolos [23], and other complex polarization distributions. Also, the fields in complex media are of interest [24–26].

The next step is to introduce the singularity of the Poynting vector (*Poynting singularity*). It has been introduced in work [27] to study the paraxial light beams. In the present paper, we do not use the approximations and consider the general three-dimensional distribution of the energy flow density vectors. Poynting vector is a real vector, and so it has no phase singularities. The Poynting singularity is caused by the indeterminacy of its direction at zero magnitude. Poynting vector is a composite quantity consisting of the electric and magnetic fields. Therefore, the Poynting singularity can appear both due to the vector field singularities (zeroes of the electric and magnetic fields) and mutual polarization of the fields (*per se*, owing to vector product). Reasoning from the said above, we introduce the terms *electric-field-induced* singularity ($\mathbf{E}=\mathbf{0}$ and $\mathbf{S}=\mathbf{0}$), *magnetic-field-induced* singularity ($\mathbf{H}=\mathbf{0}$ and $\mathbf{S}=\mathbf{0}$), and *polarization-induced* singularity ($\mathbf{E}\neq\mathbf{0}$, $\mathbf{H}\neq\mathbf{0}$, and $\mathbf{S}=\mathbf{0}$).

The Poynting singularities are necessary to study for the following reasons: (i) the measured characteristics are rather intensities (energy flows falling normally onto the detector surface) than fields and the singularities are in the realistic three-dimensional space, (ii) Poynting singularity is more generic than the phase one because it contains the phase singularities of both electric and magnetic fields therein (as Riemann-Silberstain vector [28–30]), and (iii) there exists another sort of singularity caused by the special polarization of the electromagnetic field. Note that we cannot distinguish phase singularity and polarization-induced singularity in the map of energy flow densities.

The feature of the current work is the close analogy with the theory of dynamic systems. This analogy allows investigating many problems (determining the type of singularity, dynamics of the distribution of the energy flow density, and bifurcations) and finding a number of the new topics to be studied (existence of the limit cycles or chaotic dynamics). In the "dynamic" consideration, the picture of the three-dimensional distribution of the Poynting vector is replaced with the manifold of the line trajectories of the image point. Its initial position sets the following movement under the influence of the applied energy flow density vector.

In Sec. II, the origins of the similarity of the singular optics and the theory of dynamic systems are demonstrated. The basic equation for the "optical dynamic systems" (1) is discussed. In Sec. III, the difference between the field-induced and polarization-induced singularities is shown. Also, all the field polarizations resulting in $\mathbf{S}=\mathbf{0}$ are determined. Section IV is devoted to the study of movement of the optical dynamic system in the vicinity of the singular point, line, or surface. The trajectories of the image point in the vector Bessel beam energy flow are determined as instance. The types of the singularities (vortices, focuses, nodes, and saddles) are classified in the reduced two-dimensional (2D) system considered in Sec. V. We find the types of Poynting singularities in general, without using certain field distributions. So, for the generic x-polarized magnetic field, the magnetic-field-induced singularity can be vortex, focus, or node (sink or source), while any electric-field-induced singularity is saddle. The very promising is seemed to be Sec. VI, where the tangential bifurcation is of interest. The bifurcation diagram is quite unusual and consists of several branches, which set the dynamics of the appearance or disappearance of the singularities.

II. OPTICAL DYNAMIC SYSTEMS

The Poynting vector $\mathbf{S}=(c/8\pi)\mathrm{Re}(\mathbf{E}\times\mathbf{H}^*)$ (energy flux density of the beam) represents the real vector field in the three-dimensional (physical) space. Vectors $\mathbf{E}$ and $\mathbf{H}$ are called electric and magnetic field vectors and the superscript * is for the complex conjugate. If radius vector $\mathbf{r}=(x,y,z)$ determines position of the image point on a curve and $\mathbf{S}$ is the tangent vector to this curve (see Fig. 1), then

$$\frac{d\mathbf{r}}{d\tau}\equiv\dot{\mathbf{r}}=\mathbf{S}(\mathbf{r}). \tag{1}$$

Equation (1) is the same as that for a dynamic system [31]. We introduce a fictitious point, which moves according to the equation of motion (1) with "time" τ. Parameter τ is not the genuine time; it is used just to parametrize the curve and has the dimension $[\mathbf{r}]/[\mathbf{S}]$. We suppose that S_n component shifts the image point in direction of vector $\mathbf{n}$. Since Eq. (1) does not follow from any physical problem, it is not unique. The equation $\dot{\mathbf{r}}=-\mathbf{S}(\mathbf{r})$ is of use as well. It can be reduced to Eq. (1) by the replacement $\tau\to-\tau$. Therefore, the stability cannot be studied for the image point. The stability can be considered only if the problem will be extended, e.g., using the physical reasons. Since we consider the lines of vector Poynting (not negative $\mathbf{S}$), we accept Eq. (1) and the forward direction of time from zero to infinity.

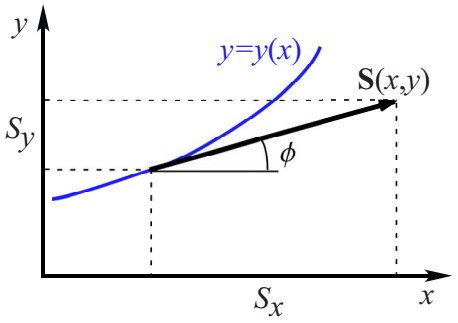

FIG. 1. (Color online) Two-dimensional plot to prove relation (1). Since $\mathbf{S}$ is the vector tangential to the curve $y=y(x)$, $\tan\phi=S_y/S_x$. On the other hand, the angle of the tangent to the curve equals $\tan\phi=dy/dx$. So, we have the expression $dy/dx=S_y/S_x$, which after parametrizing is turned to Eq. (1).

Dynamic systems are usually investigated in the phase space (in the space of momenta and coordinates of the true space), where the equations of motion are the differential equations of the first order. In the present consideration, the dimension of our "phase" space equals 3, and the space coincides with physical three-dimensional one. This corresponds to the dynamic system of the order 3/2. The example of such a system is the system of Lorentzian attractor.

Equation (1) describes the countless infinite number of lines in the three-dimensional space. These lines serve to study the structure of the field distribution during its propagation. Each line is defined by the initial conditions at the time moment $\tau=0$, i.e., by $\mathbf{r}(0)$. As the field propagates further, the parameter τ increases and the coordinates of the image point are calculated using Eq. (1).

The phase volume is simply the unit volume of the physical space: $\Gamma=dxdydz$. The speed of change in the volume can be written as

$$\dot{\Gamma}=\left(\frac{\partial\dot{x}}{\partial x}+\frac{\partial\dot{y}}{\partial y}+\frac{\partial\dot{z}}{\partial z}\right)\Gamma=\left(\frac{\partial S_x}{\partial x}+\frac{\partial S_y}{\partial y}+\frac{\partial S_z}{\partial z}\right)\Gamma=\mathrm{div}\,\mathbf{S}\Gamma. \tag{2}$$

The phase volume does not change, if $\mathrm{div}\,\mathbf{S}=\mathrm{div}\,\dot{\mathbf{r}}=0$. This equation can be fulfilled for the nondiffraction beam (such as the plane wave or Bessel beam) because nondiffraction means $\mathrm{div}\,\mathbf{S}_T=0$, where $\mathbf{S}_T$ is the Poynting vector in the direction orthogonal to the propagation direction of the beam [32]. In some situations (for example, for Bessel beams) $\mathrm{div}\,\mathbf{S}_T=\mathrm{div}\,\mathbf{S}$ and the volume is conserved. The condition

div $\mathbf{S}=0$ corresponds to Hamiltonian dynamic systems, for which the phase volume is the integral of motion. Let us consider, as what follows from div $\mathbf{S}=0$, if it is transformed using the definition of the Poynting vector and Maxwell's equations for the monochromatic waves in an anisotropic medium,

$$\nabla \times \mathbf{E} = ik_0 \varepsilon \mathbf{H}, \quad \nabla \times \mathbf{H} = -ik_0 \mu \mathbf{E}, \tag{3}$$

where $k_0=\omega/c$ is the wave number in vacuum, ω is the circular frequency, ε and μ are the dielectric permittivity and magnetic permeability tensors, respectively. Then we derive

$$\text{div } \mathbf{S} = \frac{ik_0 c}{8\pi}[\mathbf{H}(\varepsilon - \varepsilon^+)\mathbf{H}^* + \mathbf{E}^*(\mu - \mu^+)\mathbf{E}]. \tag{4}$$

The superscript + denotes the Hermitian conjugate. Now it is easily observed that the phase volume is conserved (div $\mathbf{S}=0$), if $\varepsilon=\varepsilon^+$ and $\mu=\mu^+$, i.e., for *nonabsorptive* media. Therefore, the phase volume changes only for absorptive materials, i.e., for dissipative dynamic systems.

The general solution of Eq. (2) is expressed by means of an exponent,

$$\Gamma(\tau) = \Gamma_0 \exp\left[\int_0^\tau d\tau \, \text{div } \mathbf{S}(\mathbf{r}(\tau))\right] \equiv \Gamma_0 \exp[h_\Gamma(\tau)]. \tag{5}$$

The phase volume decreases, if $h_\Gamma<0$. If the above inequality is satisfied for all $\tau>0$, the phase volume exponentially goes to zero and the phase trajectory is pulled to an attractor.

Returning to Eq. (1) we state that it is a nonlinear vector equation written in coordinate-free (covariant) form. This equation can be written in different coordinate systems, e.g., in Cartesian coordinates as

$$\dot{x} = S_x(x,y,z), \quad \dot{y} = S_y(x,y,z), \quad \dot{z} = S_z(x,y,z). \tag{6}$$

In general, in the arbitrary curvilinear coordinates (x_1,x_2,x_3) one reads

$$h_i \dot{x}_i = S_i(x_1,x_2,x_3), \quad i = 1,2,3, \tag{7}$$

where h_1, h_2, and h_3 are the Lame coefficients and S_1, S_2, and S_3 are the projections of the Poynting vector onto the basis vectors of curvilinear coordinates.

III. FIELD-INDUCED AND POLARIZATION-INDUCED SINGULARITIES

The optical Poynting singularity is defined as the point $\mathbf{r}_0$, at which the time-averaged Poynting vector becomes zero; that is,

$$\mathbf{S}(\mathbf{r}_0) = \mathbf{0}. \tag{8}$$

Using the analogy with the theory of dynamic systems, we may interpret this condition as the point, at which the image point is immovable: $\dot{\mathbf{r}}=\mathbf{0}$. These balance points can be stable or unstable and can be classified as well known.

Condition (8) puts some restrictions on the electric and magnetic fields of the beam, which are derived below. We start with the substitution of the Poynting vector definition into relation (8), which results in the equation (further we omit the dependence on $\mathbf{r}_0$)

$$\mathbf{E} \times \mathbf{H}^* + \mathbf{E}^* \times \mathbf{H} = \mathbf{0}. \tag{9}$$

Our aim is to find the magnetic field vector $\mathbf{H}$, if the electric strength $\mathbf{E}$ is known. This should give the link between the electric and magnetic fields.

Let us multiply Eq. (9) by the electric field $\mathbf{E}$,

$$[\mathbf{E} \times \mathbf{E}^*]\mathbf{H} = \mathbf{0}. \tag{10}$$

The obtained equation offers two possibilities:

(i) $[\mathbf{E}\times\mathbf{E}^*]=\mathbf{0}$. Representing $\mathbf{E}=\mathbf{E}_1+i\mathbf{E}_2$, we get from $[\mathbf{E}_1\times\mathbf{E}_2]=\mathbf{0}$ that real vectors $\mathbf{E}_1$ and $\mathbf{E}_2$ are parallel. Therefore, electric field is linearly polarized: $\mathbf{E}=\alpha\mathbf{E}_1$, where α is a complex number. One more presentation for the linearly polarized vector $\mathbf{E}$ is $\alpha\mathbf{E}^*=\alpha^*\mathbf{E}$. Now we substitute the electric field into Eq. (9): $\mathbf{E}_1\times(\alpha\mathbf{H}^*+\alpha^*\mathbf{H})=\mathbf{0}$, from which it follows

$$\alpha\mathbf{H}^* + \alpha^*\mathbf{H} = \beta\mathbf{E}_1, \tag{11}$$

where β is a real coefficient. For $\beta=0$ the special case follows: $\alpha\mathbf{H}^*=-\alpha^*\mathbf{H}$; that is, the magnetic vector is linearly polarized as well.

(ii) $[\mathbf{E}\times\mathbf{E}^*]\neq\mathbf{0}$ and $[\mathbf{E}\times\mathbf{E}^*]\mathbf{H}=\mathbf{0}$. If the electric field is nonlinearly (circularly or elliptically) polarized, then magnetic field is perpendicular to the vector $[\mathbf{E}\times\mathbf{E}^*]$. Three nonparallel complex vectors $\mathbf{E}$, $\mathbf{E}^*$, and $[\mathbf{E}\times\mathbf{E}^*]$ form the basis in three-dimensional space. Therefore, an arbitrary vector can be written as the superposition of these three basis vectors. The magnetic field then has no $[\mathbf{E}\times\mathbf{E}^*]$ projection and equals $\mathbf{H}=\alpha_1\mathbf{E}+\alpha_2\mathbf{E}^*$, where α_1 and α_2 are complex numbers. By substituting the calculated magnetic field into Eq. (9), one obtains

$$\alpha_1^*[\mathbf{E} \times \mathbf{E}^*] + \alpha_1[\mathbf{E}^* \times \mathbf{E}] = \mathbf{0}. \tag{12}$$

Since $[\mathbf{E}\times\mathbf{E}^*]\neq\mathbf{0}$, we conclude that $\alpha_1=\alpha_1^*$ is a real number. Some special cases are (a) $\alpha_1=0$, then $\mathbf{H}=\alpha_2\mathbf{E}^*$ and magnetic field is parallel to the complex conjugate electric field and (b) $\alpha_2=0$, then $\mathbf{H}=\alpha_1\mathbf{E}$ and magnetic field is parallel to the electric field.

The same formulas can be obtained provided the replacement of $\mathbf{E}$ with $\mathbf{H}$ and $\mathbf{H}$ with $\mathbf{E}$. Hence all the conditions that lead to singularity (8) can be gathered to the following list:

(1) $\mathbf{E}$ is linearly polarized as $\mathbf{E}=\alpha\mathbf{E}_1$, and $\alpha\mathbf{H}^*+\alpha^*\mathbf{H}=\beta\mathbf{E}_1$ (α is a complex number and β and $\mathbf{E}_1$ are real quantities).

(2) $\mathbf{H}$ is linearly polarized as $\mathbf{H}=\alpha\mathbf{H}_1$, and $\alpha\mathbf{E}^*+\alpha^*\mathbf{E}=\beta\mathbf{H}_1$ (α is a complex number and β and $\mathbf{H}_1$ are real quantities).

(3) $\mathbf{E}$ is circularly or elliptically polarized ($[\mathbf{E}\times\mathbf{E}^*]\neq\mathbf{0}$), and $\mathbf{H}=\alpha_1\mathbf{E}+\alpha_2\mathbf{E}^*$ (α_1 and α_2 are real and complex numbers, respectively).

(4) $\mathbf{H}$ is circularly or elliptically polarized ($[\mathbf{H}\times\mathbf{H}^*]\neq\mathbf{0}$), and $\mathbf{E}=\alpha_1\mathbf{H}+\alpha_2\mathbf{H}^*$ (α_1 and α_2 are real and complex numbers, respectively).

(5) Electric or magnetic field is equal to zero: $\mathbf{E}=\mathbf{0}$ or $\mathbf{H}=\mathbf{0}$.

It should be noted that α, α_1, α_2, β, $\mathbf{E}$, and $\mathbf{H}$ can be functions of the singularity position $\mathbf{r}_0$.

Equations in the above list can be solved for a certain medium. For instance, in an isotropic medium the magnetic field takes the form $\mathbf{H}=[-i/(k_0\varepsilon)]\nabla\times\mathbf{E}$ (Maxwell's equations) and the third condition is the differential equation

$$\nabla\times\mathbf{E}=ik_0\varepsilon(\alpha_1\mathbf{E}+\alpha_2\mathbf{E}^*). \tag{13}$$

This is the generalized equation for Beltrami fields [33,34] (the conventional equation is $\nabla\times\mathbf{E}=\alpha\mathbf{E}$). It is not surprising that at the singular point the field should be of Beltrami type because it is well known that among the solutions of the Beltrami equation the standing waves characterized by the zero energy flux density can be found. More complex electric field equations for the singularities follow for anisotropic materials.

Items (1)–(4) of the list can be joined together because they result at the singularity due to the specific polarization of the fields in the point. Therefore, we call this type of singularity as polarization-induced one. Field-induced singularities (phase singularities of the vector fields) are described by item (5). The concept of singularity is often connected with the field-induced points, which provide zero electric or magnetic field and nondefined phase. The examples of these points will be given in Sec. V. In this section, we demonstrate the idea of polarization singularity.

Example

Polarization singularity arises in the system of a vector Bessel beam of the order m in isotropic nonabsorbing medium with real dielectric permittivity ε and magnetic permeability μ. The beam moves in the z direction. We use the derived earlier (e.g., see [35,36]) electromagnetic field (solution of the Maxwell equations in cylindrical coordinates r, φ, and z),

$$\mathbf{E}(\mathbf{r},t)=e^{i\phi}\left[J_m(qr)c_2\mathbf{e}_z-\frac{k_0\mu}{q}c_1(\mathbf{e}_z\times\mathbf{b})+\frac{\beta}{q}c_2\mathbf{b}\right],$$

$$\mathbf{H}(\mathbf{r},t)=e^{i\phi}\left[J_m(qr)c_1\mathbf{e}_z+\frac{\beta}{q}c_1\mathbf{b}+\frac{k_0\varepsilon}{q}c_2(\mathbf{e}_z\times\mathbf{b})\right], \tag{14}$$

where c_1 and c_2 are the amplitudes of TE and TM partial Bessel beams, q is the transverse wave number (projection of the wave vector onto the plane orthogonal to z axis), $\beta=\sqrt{k_0^2\varepsilon\mu-q^2}$ is the longitudinal wave number (along the z axis), and $\phi=m\varphi+\beta z-\omega t$ is the Bessel beam's phase,

$$\mathbf{b}=iJ'_m(qr)\mathbf{e}_r-\frac{m}{qr}J_m(qr)\mathbf{e}_\varphi,\quad J'_m(qr)=\frac{dJ_m}{d(qr)}.$$

The Poynting vector has two nonvanishing components: longitudinal and azimuthal,

$$\mathbf{S}=\frac{c}{8\pi}\left[\frac{k_0\beta}{q^2}(\mu|c_1|^2+\varepsilon|c_2|^2)\left(J'^2_m+\frac{m^2}{q^2r^2}J_m^2\right)-\frac{2m}{q^3r}(\beta^2+k_0^2\varepsilon\mu)\mathrm{Im}(c_1c_2^*)J'_mJ_m\right]\mathbf{e}_z+\frac{c}{8\pi}\left[\frac{mk_0}{q^2r}(\mu|c_1|^2+\varepsilon|c_2|^2)J_m^2-\frac{2\beta}{q}\mathrm{Im}(c_1c_2^*)J'_mJ_m\right]\mathbf{e}_\varphi. \tag{15}$$

The Bessel beam system in nonabsorbing media is the example of Hamiltonian (conservative) system because $\mathrm{div}\,\mathbf{S}=0$. Both components of the energy flux density depend only on the radial coordinate r. We search the singularity from the conditions $S_\varphi=0$ and $S_z=0$. For $m\neq0$ they can be reduced to the couple of equations

$$(-\beta\pm k_0\sqrt{\varepsilon\mu})J_{m-1}(qr)+(\beta\pm k_0\sqrt{\varepsilon\mu})J_{m+1}(qr)=0, \tag{16}$$

$$\mu|c_1|^2+\varepsilon|c_2|^2\mp2\sqrt{\varepsilon\mu}\,\mathrm{Im}(c_1c_2^*)=0. \tag{17}$$

The first equation defines the positions of the singularities, with the position values being independent on the initial conditions (complex amplitudes c_1 and c_2). It is evident that the singularity position is determined only by the radial coordinate. Therefore, the singularity is described by the equation $r=r_0$ (with any φ and z). The amplitudes c_1 and c_2 are not arbitrary. They are very specific and can be extracted from Eq. (17). Putting Eqs. (16) and (17) into the field expressions (14), we get to the fields at a singular point,

$$\mathbf{H}=\frac{c_1}{c_2}\mathbf{E},$$

$$\mathbf{E}=e^{i\phi}c_2\left[-\frac{\beta\pm k_0\sqrt{\varepsilon\mu}}{q}J_{m+1}(qr_0)\mathbf{e}_\varphi+J_m(qr_0)\mathbf{e}_z\right]. \tag{18}$$

One notes that in spite of zero Poynting vector, neither electrical nor magnetic field equals zero. The singularity is generated due to the colinearity of the electric and magnetic field strengths (specific polarization of the vector beam). Since $\mathbf{E}\times\mathbf{E}^*=\mathbf{0}$ and $\mathbf{H}\times\mathbf{H}^*=\mathbf{0}$, both electric and magnetic fields are linearly polarized and our polarization singularity belongs to the first or second item of the list presented above ($\beta=\mathbf{0}$). Nonlinearly polarized fields at the singular points can be obtained for evanescent vector Bessel beams [37]. Such singularities satisfy the third item of the list.

IV. SINGULAR POINTS, LINES, AND SURFACES

The further study of optical dynamic systems implies the linearization of the existing nonlinear equations near the singular point $\mathbf{r}_0$. Since $\mathbf{S}(\mathbf{r})\approx\mathbf{S}(\mathbf{r}_0)+(\delta\mathbf{r}\nabla_0)\mathbf{S}(\mathbf{r}_0)$ and $\mathbf{S}(\mathbf{r}_0)=\mathbf{0}$, we find

$$\dot{\delta}\mathbf{r}=(\delta\mathbf{r}\nabla_0)\mathbf{S}(\mathbf{r}_0)\equiv\delta\mathbf{r}[\nabla_0\otimes\mathbf{S}(\mathbf{r}_0)], \tag{19}$$

where $\nabla_0=\partial/\partial\mathbf{r}_0$ and $\delta\mathbf{r}=\mathbf{r}-\mathbf{r}_0$. Vector (19) is linear with constant matrix coefficient

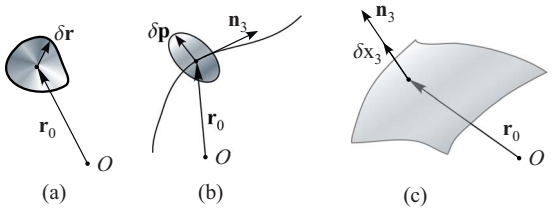

FIG. 2. (Color online) (a) Three-dimensional, (b) two-dimensional, and (c) one-dimensional vicinity of the isolated singular point, singular line, and singular surface, respectively.

$$G = \nabla_0 \otimes \mathbf{S}(\mathbf{r}_0). \tag{20}$$

In the above equation, the 3×3 stability matrix G is coordinate free. It can be rewritten in Cartesian coordinates as $G_{ij}=\partial S_j/\partial x_i^0$, or in curvilinear coordinates as

$$G = \sum_{i,j=1}^{3} \frac{1}{h_i}\frac{\partial S_j}{\partial x_i^0}\mathbf{e}_i \otimes \mathbf{e}_j + \sum_{i,j=1}^{3} \frac{S_j}{h_i}\mathbf{e}_i \otimes \frac{\partial \mathbf{e}_j}{\partial x_i^0}, \tag{21}$$

where $\mathbf{e}_i$ are the basis vectors of the curvilinear coordinates. If we use G in curvilinear coordinates, we should take the vector $\delta\mathbf{r}$ in the same basis, so that linear equation (19) will be converted to the nonlinear one.

In the further consideration, we should distinguish the situations when the singularity is an isolated point or line or surface in three-dimensional space (Fig. 2). For the isolated singular point, the surrounding points are identical (not singular). Therefore, the problem to be solved is three dimensional and the covariant solution of Eq. (19) is of the form

$$\mathbf{r} = \mathbf{r}_0 + \delta\mathbf{r}_0 \exp(G\tau). \tag{22}$$

The stability matrix can be presented in the spectral form $G=\lambda_1\rho_1+\lambda_2\rho_2+\lambda_3\rho_3$, where λ_i and ρ_i $(i=1,2,3)$ are the eigenvalues and projection operators onto the eigenvectors of the matrix G. Projectors possess the following properties: $\rho_1+\rho_2+\rho_3=\mathbf{1}$ and $\rho_i\rho_j=\rho_i\delta_{ij}$, where $\mathbf{1}$ is the unit three-dimensional matrix and δ_{ij} is the Kronecker delta. The projector can be written as the outer product of the eigenvector $\mathbf{v}$ of G and eigenvector $\mathbf{u}$ of the transposed matrix G^T: $\rho_i=\mathbf{u}_i\otimes\mathbf{v}_i$. Then, expression (22) takes the form

$$\mathbf{r} = \mathbf{r}_0 + \delta\mathbf{r}_0(e^{\lambda_1\tau}\rho_1 + e^{\lambda_2\tau}\rho_2 + e^{\lambda_3\tau}\rho_3). \tag{23}$$

For increasing τ, the radius vector $\mathbf{r}$ will tend to $\mathbf{r}_0$ only if all the real parts of eigenvalues are negative: $\mathrm{Re}\,\lambda_i<0, i=1,2,3$. This is possible only for dissipative dynamic systems. In fact, the condition of a conservative (Hamiltonian) system is $\mathrm{div}\,\mathbf{S}=\mathbf{0}$ [see the discussion after Eq. (2)]. In the vicinity of the singular point, we compute $\mathrm{div}\,\mathbf{S}=\mathrm{div}(\delta\mathbf{r}G)=\mathrm{Tr}(G)=\lambda_1+\lambda_2+\lambda_3$ and make sure that $\mathrm{div}\,\mathbf{S}\neq\mathbf{0}$, if $\mathrm{Re}\,\lambda_i<0$.

For Hamiltonian systems, there exists the generalized Toda's criterion of local instability [38]. Two conclusions follow from this criterion:

(i) the local instability of the movement arises, if $\mathrm{Re}\,\lambda_i\neq 0$ for some i. Since the phase volume is constant, the compression of the phase flux in one direction (e.g., $\mathrm{Re}\,\lambda_1<0$) is accompanied with its stretching in another one ($\mathrm{Re}\,\lambda_2>0$); and

(ii) if $\mathrm{Re}\,\lambda_i=0$ for any $i=1,2,3$, then the motion of the image point is stable and regular.

Thus, the dynamics of the image point can be both regular and stochastic depending on the eigenvalues of the stability matrix [39].

Another situation arises, when the singularities are distributed along the line. Then the nonsingular points near the line are situated in the plane perpendicular to this line and described by the in-plane radius vector $\mathbf{p}=\mathbf{r}-(\mathbf{r}\mathbf{n}_3)\mathbf{n}_3$, where $\mathbf{n}_3$ is the unit tangent vector to the line [Fig. 2(b)]. Therefore, we get to the two-dimensional equation for $\mathbf{p}$,

$$\dot{\mathbf{p}} = \dot{\mathbf{r}} - (\dot{\mathbf{r}}\mathbf{n}_3)\mathbf{n}_3 = \mathbf{S} - (\mathbf{S}\mathbf{n}_3)\mathbf{n}_3 = \mathbf{S}_\perp(\mathbf{r}). \tag{24}$$

The in-plane Poynting vector $\mathbf{S}_\perp$ near the singular line can be expanded to a series, with the variations of coordinates being in the plane perpendicular to the line: $\mathbf{S}_\perp(\mathbf{r}) \approx \mathbf{S}_\perp(\mathbf{r}_0)+(\delta\mathbf{p}\,\partial/\partial\mathbf{p}_0)\mathbf{S}_\perp(\mathbf{r}_0)$. Using the expansion to the series for $\mathbf{S}_\perp$, the equation near the singular line can be derived as follows:

$$\dot{\delta\mathbf{p}} = \left(\delta\mathbf{p}\frac{\partial}{\partial\mathbf{p}_0}\right)\mathbf{S}_\perp(\mathbf{r}_0), \tag{25}$$

where $\delta\mathbf{p}=\mathbf{p}-\mathbf{p}_0$. The stability matrix $G=\partial/\partial\mathbf{p}_0\otimes\mathbf{S}_\perp(\mathbf{r}_0)$ is two dimensional now: Eq. (25) contains only two components of the Poynting vector and only two coordinates. The 2D case is well investigated in many papers because it provides the analysis of the types of singularities (vortices, sources, sinks, and saddles). The third coordinate x_3 changes according to the equation

$$\delta\dot{x}_3 = (\mathbf{S}\mathbf{n}_3) = \delta\mathbf{p}\frac{\partial S_3(\mathbf{r}_0)}{\partial\mathbf{p}_0}, \tag{26}$$

which can be integrated, if $\delta\mathbf{p}$ is found from Eq. (25).

Let us consider the situation when there is the surface of singularities in the three-dimensional space [Fig. 2(c)]. Nonsingular points are placed on the lines perpendicular to this surface: $x_3=\mathbf{r}\mathbf{n}_3$ is the coordinate along the line, where $\mathbf{n}_3$ is the unit vector normal to the surface. The equation of motion for the coordinate x_3 in the vicinity of the singular surface is one dimensional, i.e.,

$$\dot{\delta x}_3 = \delta x_3\frac{\partial[\mathbf{n}_3\mathbf{S}(\mathbf{r}_0)]}{\partial x_3^0}. \tag{27}$$

Here the assertion that the Poynting vector can change only along the direction orthogonal to the singular surface is used. The other coordinates x_1 and x_2, joined into the vector $\mathbf{p}$, can be computed from the equation

$$\dot{\delta\mathbf{p}} = \delta x_3\frac{\partial\mathbf{S}_\perp(\mathbf{r}_0)}{\partial x_3^0}. \tag{28}$$

Equations (27) and (28) are easily solved with regard to the trajectory of the image point $\mathbf{r}(\tau)=\mathbf{r}_0+\delta\mathbf{p}(\tau)+\mathbf{n}_3\delta x_3(\tau)$ as follows:

$$\mathbf{r}(\tau) = \mathbf{r}_0 + \frac{1}{\lambda}\frac{\partial \mathbf{S}(\mathbf{r}_0)}{\partial x_3^0} e^{\lambda\tau}\delta x_3(0) - \frac{1}{\lambda}\frac{\partial \mathbf{S}_\perp(\mathbf{r}_0)}{\partial x_3^0}\delta x_3(0). \quad (29)$$

The stable singular point follows from the condition $\lambda = \partial S_3(\mathbf{r}_0)/\partial x_3^0 < 0$ (λ is always real quantity). We suppose that the initial position of the image point is $\mathbf{r}_0 + \mathbf{n}_3\delta x_3(0)$, so that the quantity $\delta x_3(0)$ defines the initial position of the image point in the coordinate frame regarding the singularity $\mathbf{r}_0$. Equation (29) represents the movement of the image point in the plane tangent to the singular surface at the point $\mathbf{r}_0$ (*per se*, in the plane involute of the singular surface). Therefore, if (x_1, x_2, x_3) are the orthogonal coordinates at $\mathbf{r}_0$, then

$$\mathbf{r}(\tau) = \mathbf{r}_0 + \sum_{i=1}^{3} h_i(\tau)\delta x_i(\tau)\mathbf{n}_i, \quad (30)$$

where $\mathbf{n}_1$ and $\mathbf{n}_2$ are the unit vectors in the tangent plane and Lame coefficients h_i can also depend on the coordinates and, hence, on τ. Equation (30) defines τ dependencies of the curvilinear coordinates. Vectors $\mathbf{n}_i$ point out the directions of the change in coordinates (in and out the singular surface). The same solution can be derived, if Eq. (19) is directly solved in curvilinear coordinates. Then the vector equation comes apart as

$$h_i\dot{\delta}x_i = \frac{\partial S_i(x_1^0, x_2^0, x_3^0)}{\partial x_3^0}\delta x_3, \quad i = 1,2,3. \quad (31)$$

The relation div $\mathbf{S} = \lambda = 0$ corresponds to Hamiltonian (conservative) dynamic systems. This special case results in the simple solution

$$\mathbf{r}(\tau) = \mathbf{r}_0 + \left[\frac{\partial \mathbf{S}_\perp(\mathbf{r}_0)}{\partial x_3^0}\tau + \mathbf{n}_3\right]\delta x_3(0), \quad (32)$$

which means that near the singular surface coordinate x_3 is constant, while the vector along the surface changes linearly. For example, if the singular surface is $z = \text{const}$ in Cartesian coordinates, then the image point moves along the straight line. The trajectory of the point repeats the form of the singular surface. Therefore, the movement of the particle is regular and the singularity is of the center type (there is no trajectories that go through the singularities). Below the example in cylindrical coordinates is considered.

We also define a zero-dimensional (0D) problem as the situation when the whole space is filled with the singular points. The aim is to determine the electromagnetic fields that has zero Poynting vector at every point of the three-dimensional space. Such a problem can be solved using the list of relations (1)–(4) obtained earlier in this section. Beltrami field is the special case of 0D problem.

Example

Here we continue the investigation of vector Bessel beam singularities. In Sec. III we have defined the positions of the singular points. Radial coordinates of these points satisfy Eq. (16), while φ and z can take arbitrary values. Hence we guess that the singular points are situated at the surface $r = r_0$, where r_0 is the root of Eq. (16). Now we will apply the general analysis developed above.

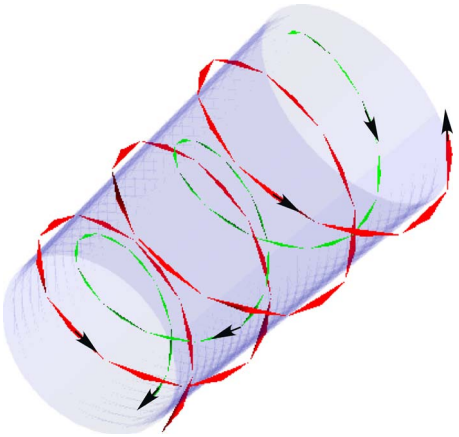

FIG. 3. (Color online) Spiral trajectories of the image point. The singular surface is the cylinder of radius r_0. Since at the singularity the Poynting vector $\mathbf{S}$ changes the sign, the spirals near r_0, at $r > r_0$ (red) and $r < r_0$ (green), will be directed oppositely.

In the considered system, coordinate x_3 is the radial coordinate r, while the unit radial vector $\mathbf{e}_r$ is the normal vector to the singular surface $\mathbf{n}_3$. Since Bessel beam field in a non-absorbing medium corresponds to the Hamiltonian dynamic system, we write div $\mathbf{S} = \lambda = 0$. Thus, from expression (32) the trajectory of the image point follows

$$\mathbf{r}(\tau) = \mathbf{r}_0 + \mathbf{e}_r\delta r(0) + \tau\left[\frac{\partial S_\varphi(r_0)}{\partial r_0}\mathbf{e}_\varphi + \frac{\partial S_z(r_0)}{\partial r_0}\mathbf{e}_z\right]\delta r(0), \quad (33)$$

where $\mathbf{S}_\perp = S_\varphi\mathbf{e}_\varphi + S_z\mathbf{e}_z$. The derivatives can be calculated using the explicit expression for the Poynting vector (15) and the equations defining the singularities (16) and (17). However, the trajectory of the image point can be estimated from the already obtained equation (33). The point linearly shifts in azimuthal and longitudinal directions: the image point spires. According to Eqs. (30) and (33) we find $\delta r = \delta r(0)$, $\delta\varphi = \tau\partial S_\varphi/\partial r_0$, and $\delta z = \tau\delta r(0)\,\partial S_z/\partial r_0$. Since δr is constant, the point moves at the fixed distance from the singular cylindrical surface. The initial position of the point $\mathbf{r}_0 + \mathbf{e}_r\delta r(0)$ specifies the certain spiral trajectory, so that the different spirals cover all the space without intersections.

For the vector Bessel beams, there exist the spatial regions, where the Poynting vector $\mathbf{S}$ is pointed to the opposite propagation direction of the beam (the case of the so-called negative propagation [35,40] when the longitudinal component S_z is negative). The singular surfaces divide the regions of negative and positive propagation. The image point shifts along the z axis for positive propagation and oppositely for the negative one. This situation is demonstrated in Fig. 3.

V. TYPES OF POYNTING SINGULARITIES

In this section, we consider the singular lines in the three-dimensional space. After passing on to the two-dimensional space (to the plane perpendicular to the singular line) the lines will turn to the isolated singular points. These points can be classified as well known in the theory of dynamic

systems. So, each critical point can be center, focus, node, or saddle. Using the stability matrix G we will remind the criteria of defining the type of the point.

We start with Eq. (25) with redefined stability matrix G,

$$\dot{\delta}\mathbf{p} = G\delta\mathbf{p}, \quad G = \left[\frac{\partial}{\partial \mathbf{p}_0} \otimes \mathbf{S}_\perp(\mathbf{r}_0)\right]^{\mathrm{T}}, \tag{34}$$

where superscript T denotes the transposition. Searching for the solution of Eq. (34) in the exponential form $\delta\mathbf{p} = \exp(\lambda\tau)\mathbf{c}$, we derive the dispersion equation for λ in the form

$$\lambda^2 - G_t\lambda + |G| = 0, \tag{35}$$

where G_t and $|G|$ are the trace and determinant of the matrix G, respectively. The solutions of this quadratic equation set the type of a critical point in the plane.

So, we get the following classification of the singularities [31]:

(i) *Vortex* (center in the theory of dynamic systems) corresponds to the imaginary solutions of Eq. (35): $\lambda_1 = -\lambda_2 = i\alpha$, where α is a real number. The trajectory of the image point near the vortex is the closed elliptic curve. Vortex appears, if $G_t = 0$ and $|G| > 0$.

(ii) *Focus* (focus or spiral point in the theory of dynamic systems) corresponds to the complex conjugate solutions of Eq. (35): $\lambda_1 = \alpha + i\beta$ and $\lambda_2 = \alpha - i\beta$, where α and β are real numbers. The trajectory of the image point near the focus is the diverging or converging spiral. Stable (unstable) focus appears, if $G_t < 0$ ($G_t > 0$) and $|G| > G_t^2/4$.

(iii) *Sink* or *source* (stable or unstable node in the theory of dynamic systems) corresponds to the real like-sign solutions of Eq. (35): $\lambda_1\lambda_2 > 0$. Sink arises, when $\lambda_1 < 0$ and $\lambda_2 < 0$, while $\lambda_1 > 0$ and $\lambda_2 > 0$ is the condition for the source. The trajectories of the image point near the sink (source) are the converging (diverging) parabolas. Sink (source) appears, if $G_t < 0$ ($G_t > 0$) and $|G| < G_t^2/4$.

(iv) *Saddle* (saddle in the theory of dynamic systems) corresponds to the real opposite-sign solutions of Eq. (35): $\lambda_1\lambda_2 < 0$. The trajectories of the image point near the saddle are the hyperbolas. Saddle appears, if $|G| < 0$.

Note that the stability of the singular points is defined in this formulation. All the types of singularities can be gathered to the diagram demonstrated in Fig. 4.

Let us consider the vector beam in an absorbing isotropic material with complex dielectric permittivity $\varepsilon = \varepsilon_1 + i\varepsilon_2$ and magnetic permeability $\mu = 1$. We suppose that such a beam forms the lines of phase singularity along the Cartesian coordinate x and is characterized by the TM polarization,

$$\mathbf{H}(y,z) = H_x(y,z)\mathbf{e}_x, \quad \mathbf{E}(y,z) = E_y(y,z)\mathbf{e}_y + E_z(y,z)\mathbf{e}_z. \tag{36}$$

TE polarization follows from the mutual replacement of electric and magnetic fields. The problem to be solved is obviously two dimensional [in the plane (y,z)]. Magnetic- and electric-field-induced singularities are connected with the zeroes of the complex functions H_x or E_y and E_z, respectively. At first, we will investigate the singular points provided by the magnetic field; that is, the points $y = y_0$ and $z = 0$, at which $H_x(y_0,0) = 0$.

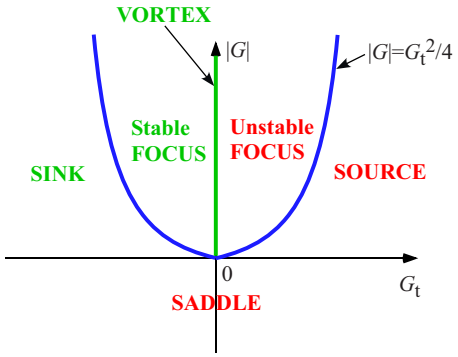

FIG. 4. (Color online) Diagram defining the type of optical singularity using the trace and the determinant of the stability matrix G.

Magnetic-field-induced Poynting singularities are defined as $\mathbf{S}(y_0,0) = \mathbf{0}$. In spite of the coincidence of the Poynting and phase singularities, the types of the points differ. The energy flux density for fields (36) equals

$$\mathbf{S}(y,z) = S_y(y,z)\mathbf{e}_y + S_z(y,z)\mathbf{e}_z,$$

$$S_y = \frac{c}{8\pi}\mathrm{Re}(E_z H_x^*), \quad S_z = -\frac{c}{8\pi}\mathrm{Re}(E_y H_x^*), \tag{37}$$

while Maxwell's equations connect electric and magnetic fields as

$$\mathbf{E} = -\frac{1}{ik_0\varepsilon}\nabla \times \mathbf{H} \equiv -\frac{1}{ik_0\varepsilon}\frac{\partial H_x}{\partial z}\mathbf{e}_y + \frac{1}{ik_0\varepsilon}\frac{\partial H_x}{\partial y}\mathbf{e}_z,$$

$$H_x = \frac{1}{ik_0}\left(\frac{\partial E_z}{\partial y} - \frac{\partial E_y}{\partial z}\right). \tag{38}$$

The magnetic field strength can be expanded into the Taylor series near the singular point $H_x(y_0,0) = 0$ as

$$H_x(y,z) \approx \left(\frac{\partial H_x}{\partial y}\right)_0 \delta y + \left(\frac{\partial H_x}{\partial z}\right)_0 \delta z, \tag{39}$$

where $\delta y = y - y_0$ and $\delta z = z - 0$ are the deviations of the coordinates from the singularity. The subscript 0 denotes that the derivatives are calculated at the point $y = y_0, z = 0$ These derivatives can be expressed through the electric field components (38) as

$$\left(\frac{\partial H_x}{\partial y}\right)_0 = ik_0\varepsilon E_z(y_0,0), \quad \left(\frac{\partial H_x}{\partial z}\right)_0 = -ik_0\varepsilon E_y(y_0,0). \tag{40}$$

Further we will omit the arguments of the electric field components. By substituting the electric $\mathbf{E}$ and magnetic $H_z = ik_0\varepsilon(E_z\delta y - E_y\delta z)$ vectors into the Poynting vector components (37), we write

$$S_y = a_{11}\delta y + a_{12}\delta z, \quad S_z = a_{21}\delta y + a_{22}\delta z, \tag{41}$$

where

$$a_{11} = -\frac{\omega}{8\pi}\varepsilon_2|E_z|^2, \quad a_{12} = \frac{\omega}{8\pi}\mathrm{Re}(i\varepsilon^* E_z E_y^*),$$

$$a_{21} = -\frac{\omega}{8\pi}\mathrm{Re}(i\varepsilon E_z E_y^*), \quad a_{22} = -\frac{\omega}{8\pi}\varepsilon_2|E_y|^2. \tag{42}$$

The types of the singular points can be determined using the trace and determinant of the stability matrix

$$G = \begin{pmatrix} a_{11} & a_{12} \\ a_{21} & a_{22} \end{pmatrix}. \tag{43}$$

The invariants of matrix G have the following form:

$$G_t = a_{11} + a_{22} = -\frac{\omega}{8\pi}\varepsilon_2(|E_y|^2 + |E_z|^2),$$

$$|G| = a_{11}a_{22} - a_{12}a_{21} = \left(\frac{\omega}{8\pi}\right)^2 |\varepsilon|^2 \,\mathrm{Im}(E_z E_y^*)^2. \tag{44}$$

Now let us address the diagram shown in Fig. 4. Since $|G|>0$, the singularity can be vortex, focus, or node. The stability is defined by the sign of the imaginary part of dielectric permittivity: at $\varepsilon_2>0$ ($\varepsilon_2<0$) the points are stable (unstable). The singular points can be identified depending on ε_2. If $\varepsilon_2=0$, then $G_t=0$ and the point is vortex. Stable focus appears, if $|G|>G_t^2/4$, i.e.,

$$2|\varepsilon||\mathrm{Im}(E_z E_y^*)| > |\varepsilon_2|(|E_y|^2 + |E_z|^2). \tag{45}$$

For the sign "less" in the inequality above the node arises. *Per se*, relation (45) is the inequality for ε_2, which enters not only into the dielectric permittivity ε, but into the electric field components as well.

Now we turn to the singularities of the electric field **E**, i.e., the points $y=y_0$ and $z=0$, at which $E_y(y_0,0)=0$ and $E_z(y_0,0)=0$. We expand the electric field in the vicinity of the singular point into the Taylor series as follows:

$$\mathbf{E} \approx \left(\frac{\partial \mathbf{E}}{\partial y}\right)_0 \delta y + \left(\frac{\partial \mathbf{E}}{\partial z}\right)_0 \delta z. \tag{46}$$

By substituting the magnetic field H_x from the Maxwell equations (38) into the expression for Poynting vector (37) and using the expression div $\mathbf{E}=\partial E_y/\partial y+\partial E_z/\partial z=0$, we get to the stability matrix G with the following real components:

$$a_{11} = -a_{22} = -\frac{c}{8\pi k_0}\mathrm{Re}\left[i\frac{\partial E_z}{\partial y}\frac{\partial E_y^*}{\partial z}\right],$$

$$a_{12} = a_{21} = \frac{c}{8\pi k_0}\mathrm{Re}\left[i\frac{\partial E_z}{\partial z}\left(\frac{\partial E_z^*}{\partial y} - \frac{\partial E_y^*}{\partial z}\right)\right]. \tag{47}$$

The determinant of the stability matrix is always negative: $|G|=-a_{11}^2-a_{12}^2<0$. Therefore, the only type of the singular point, namely, the saddle, is possible (see Fig. 4).

So, we have defined the type of the Poynting singular point without information about certain field distribution. For TE-polarized beams, we need to replace **H** with **E**, **E** with **H**, ε with $-\mu$, and μ with $-\varepsilon$. It is evident that the types of the singularities can be found in the similar way. We obtain vortex, focus, or node for the singularities of the linearly polarized electric field E_x and saddle for the singularities of the magnetic field **H**. In nonabsorbing media (as for the Hamiltonian dynamic systems) only vortices or saddles can appear.

Following the theory of dynamic systems, we need to study, whether the *limit cycles* are possible for the electromagnetic beams. The limit cycle is the singular trajectory of a dissipative system. The system cannot get to this trajectory for the finite time or come down from it, if it was situated in the trajectory at the initial time moment [31].

The dissipative system can be easily realized for the electromagnetic beam, if the absorbing medium is taken. However, it is not sufficient. The sufficient condition of the absence of the closed trajectories is provided by the Bendickson criterion, which is formulated for the two-dimensional system

$$\dot{y} = S_y(y,z), \quad \dot{z} = S_z(y,z) \tag{48}$$

as follows: if in some simply connected domain in the plane (y,z) the expression

$$\frac{\partial S_y}{\partial y} + \frac{\partial S_z}{\partial z} \equiv \mathrm{div}\ \mathbf{S}$$

is of invariable sign, then there are no closed contours (including limit cycles) in this domain, which are fully formed from the trajectories of the system.

Applied to the beams in isotropic media $\varepsilon=\varepsilon_1+i\varepsilon_2$ and $\mu=1$, the Bendickson criterion results in

$$\mathrm{div}\ \mathbf{S} = -\frac{k_0 c}{4\pi}\varepsilon_2|\mathbf{H}|^2. \tag{49}$$

This expression does not vary the sign, if the imaginary part of the dielectric permittivity is constant. However, if $\varepsilon_2=\varepsilon_2(y,z)$, then the limit cycles may appear as the singular trajectory of the image point. The change in the sign of ε_2 means that one spatial region is amplifying, while another region is absorbing. If the amplifying region is at small coordinates, then the trajectory from the initial point inside this domain will increase the coordinate going to the limit cycle. The image point from the initial point in the absorbing region will decrease the coordinates going to the limit cycle from another side. It is possible that anisotropic medium can help in creating limit cycles.

Example

A good example showing all the features of the theory provided above is the electromagnetic field generated by the magnetic field source distributed in the plane $z=0$ as $H_x(y,0)=Ay\cos(py)$, where A is an amplitude and p is a wave parameter (transverse wave number). This source is very attractive because it allows finding the closed-form expressions for electric and magnetic fields. The function $H_x(y,0)$ strongly increases in infinite limits of the coordinate y. That is why the limited coordinates y (as always in physi-

cal problems) should be considered. However, further we turn back to the mathematical formulation with nonlimited coordinates y. The chosen source contains the infinite number of phase singularities of the magnetic field, which can be found from the condition $H_x(y_0,0)=0$: $y_0=\pi(n+1/2)/p$. The situation $y=0$ is out of our interest because at this point both H_x and E_y turn to zero (it should be studied separately).

Using the Fourier method, the fields can be restored as

$$H_x(y,z) = Ae^{i\kappa z}\left[y\cos(py) - \frac{ipz}{\kappa}\sin(py)\right],$$

$$E_y(y,z) = -\frac{A}{\varepsilon k_0}e^{i\kappa z}\left[\kappa y\cos(py) - \frac{p}{\kappa}\sin(py) - ipz\sin(py)\right],$$

$$E_z(y,z) = \frac{A}{i\varepsilon k_0}e^{i\kappa z}\left[\cos(py) - py\sin(py) - \frac{ip^2}{\kappa}z\cos(py)\right], \tag{50}$$

where $\kappa=\sqrt{k_0^2\varepsilon-p^2}$ is the longitudinal wave number. Except the magnetic-field-induced phase singularities, the electric-field-induced singularities exist. They appear when both components of the electric field equal zero: $E_y(y_0,0)=E_z(y_0,0)=0$. The combined solution of this couple of equations results in only some possible transverse wave numbers p. At $p/k_0=1.0312$ two electric-field-induced singularities arise, namely, $k_0y_0=\pm 0.8343$.

Let us observe the positions of Poynting singularities. Since $S_y(y,0)=0$, in Fig. 5(a) we show the nonvanishing component $S_z(y,0)$. Poynting singularities arise for $S_z(y_0,0)=0$. From Fig. 5(a) we note that three singularities are generated by the electric or magnetic field. The rest singular point is the so-called polarization-induced singularity (due to specific polarization of the electromagnetic field). There are infinite number of pairs of singular points (saddle-vortex) along the y axis and only the first saddle is caused by the electric field vector singularity. All other saddles are owing to polarization. The distance between the vortex and saddle decreases for the remote pairs. Since $\mathbf{H}$ is linearly polarized at the point of polarization-induced singularity, electric field vector satisfies the equation $\alpha\mathbf{E}^*+\alpha^*\mathbf{E}=\beta\mathbf{H}/\alpha$ (see Sec. III). Since $\mathbf{H}$ is directed along the x axis, while $\mathbf{E}$ does not, it is necessary to put $\beta=0$ and, therefore, the electric field is linearly polarized. If magnetic field polarization is expressed as $\mathbf{H}=\alpha\mathbf{H}_1$ ($\mathbf{H}_1$ is the real part of the magnetic field and α is a complex number), then the electric field at the point of singularity must be $\mathbf{E}=i\alpha\mathbf{E}_1$ ($\mathbf{E}_1$ is the real part of the electric field). From Eq. (50) it follows that $\mathbf{H}$ is real at singularity $(y_0,0)$; hence, α is real number and $\mathbf{E}$ is the imaginary vector. This can be fulfilled only if the real component $E_y(y_0,0)=0$. Such a condition serves for finding the polarization-induced singularities y_0 at the axis z.

One more peculiarity can be noted in Fig. 5(a). The distance between the saddle and vortex is the region of negative Poynting component S_z (negative propagation of the beam according to [35]). Such negative propagation domains arise in many beam structures and are connected with the complicated interference picture of vector fields. The distances between the couple saddle-vortex diminishes with increase in the coordinate y; therefore, the regions of negative Poynting component become smaller too.

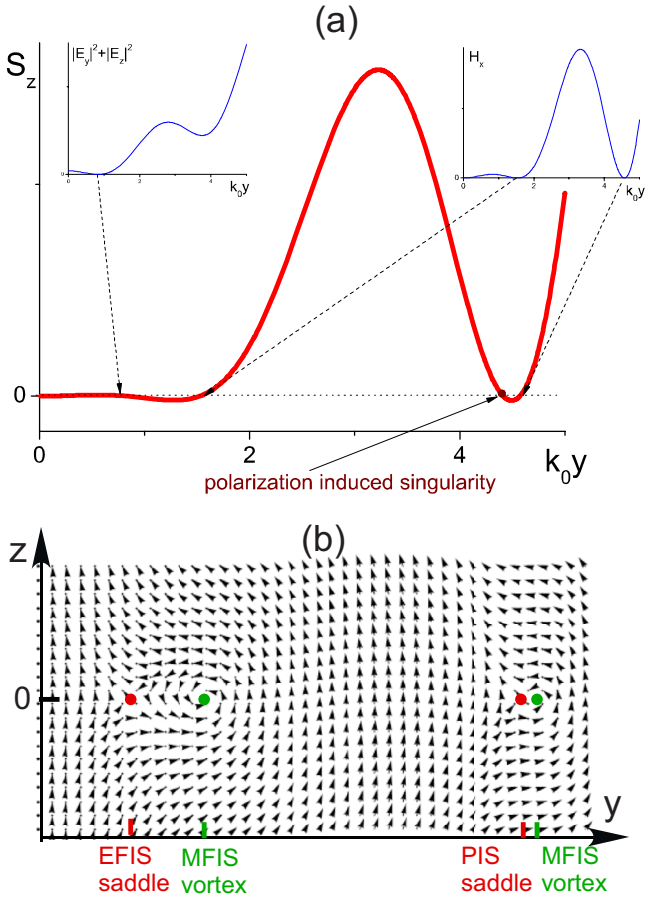

FIG. 5. (Color online) (a) The origin of the Poynting singularities for fields (50) in nonabsorbing dielectric media. For four singularities shown, we define one electric-field-induced singularity (EFIS), two magnetic-field-induced singularities (MFIS), and one polarization-induced singularity (PIS). (b) Poynting vector picture with indication of the singularity types. Parameters: $\varepsilon_1=2.5$, $\varepsilon_2=0$, and $p/k_0=1.0312$.

For the nonabsorbing media the only singular points are vortices and saddles [Fig. 5(b)]. More interesting situation arises for an absorbing medium with complex dielectric permittivity $\varepsilon=\varepsilon_1+i\varepsilon_2$. Increasing the imaginary part of the dielectric permittivity, we can achieve the transformation of the singularity type as displayed in Fig. 6. At $\varepsilon_2=0$ the possible points are (a) vortex and (d) saddle. Saddle is the electric-field-induced or polarization-induced singularity. Vortex is the singularity of the vanishing magnetic field. When ε_2 arises, vortex is converted to another stable point. If ε_2 is small enough [inequality (45) is fulfilled], (b) the stable focus appears: the image point will be attracted to this point. (c) Larger ε_2 transforms focus into the sink. Thus, the change in the system parameter affects the type of the singularity.

Evanescent waves are generated for the wave numbers p greater than $k_0\sqrt{\varepsilon\mu}$. For such waves the only type of singular point for H_x is available—it is node (sink or source). The proof of this statement for fields (50) can be made in the closed form. The singularities for evanescent waves are not the isolated points. They form the lines in the plane (y,z);

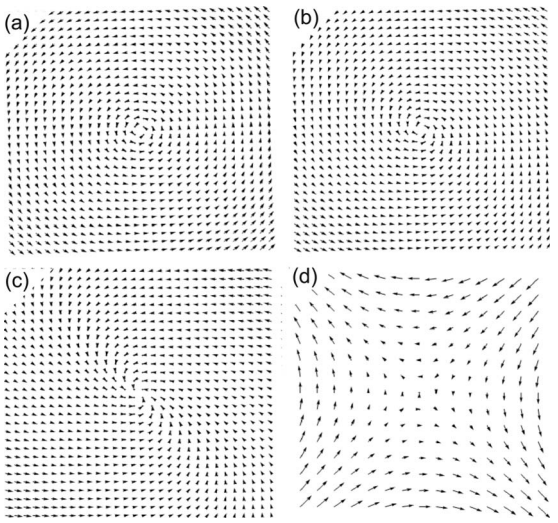

FIG. 6. Evolution of the singularity type depending on the imaginary part of dielectric permittivity ε_2: (a) vortex at $\varepsilon_2=0$, (b) stable focus at $\varepsilon_2=0.5$, and (c) sink at $\varepsilon_2=1.5$. (d) Also the saddle point is shown. Parameters: $\varepsilon_1=2.5$ and $p/k_0=1.0312$.

i.e., the singular surfaces in the three-dimensional space arise.

VI. BIFURCATIONS IN SINGULAR OPTICS

Bifurcation is any qualitative (topological) reorganization of the system at the parameter transition through a critical (branching) value. Usually bifurcations are connected with appearance or disappearance of the critical points (singularities in our interpretation).

There are some physical parameters that can be varied. We have already changed medium parameters, such as dielectric permittivity (or magnetic permeability), to see the change in the type of the singular point (see Fig. 6). But more powerful tool to bifurcate is hidden in the field parameters. In fact, in the considered system (50) the wave number parameter p strongly affects the electric-field-induced singularities. Only at some special points these singularities may appear. For another parameters p this saddle point does not exist.

The singularities can appear or disappear in couples because Poincare's index (topological charge of the electromagnetic field) should stay constant when parameter varies. At the bifurcation value, the complex critical point arises (e.g., saddle-node), which is then segregated into two (or more) isolated points with zero total index. Below we consider a simple example of Poynting bifurcations.

Example

The selected example is a sort of *tangential bifurcation*, which is generally introduced for a one-dimensional dynamic system $\dot{x}=\lambda-x^2$ [39]. We transform the system of tangential bifurcation supposing that x-polarized magnetic field depends on real parameter λ as

$$H_x(y,0)=A(\lambda-y^2), \tag{51}$$

where A is an amplitude. The source $H_x(y,0)$ itself has two singular points in the y axis, namely, $y_0=\pm\sqrt{\lambda}$. Depending on the parameter value, two situations are possible: there is no singularities ($\lambda<0$) and there are two singularities ($\lambda>0$). At $\lambda=0$, the complex singularity arises.

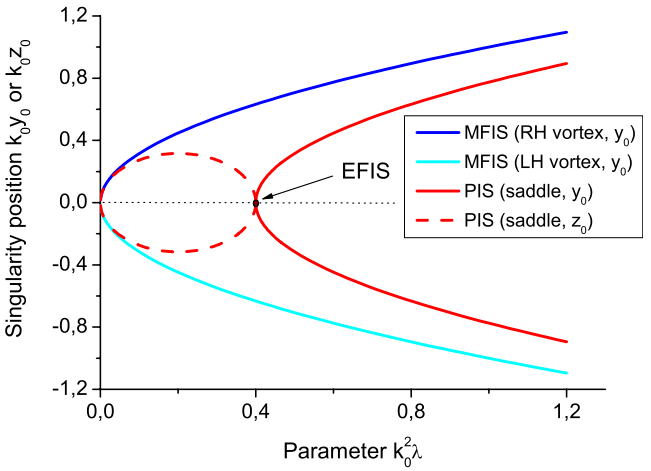

FIG. 7. (Color online) Bifurcation diagram (dependence of the singularity position on parameter λ) showing magnetic-field-induced singularity (MFIS), electric-field-induced singularity (EFIS), and polarization-induced singularity (PIS). Only dashed curve corresponds to the PIS situated in the z axis. Real dielectric permittivity equals $\varepsilon=2.5$.

For the given source, the fields can be analytically calculated as follows:

$$H_x(y,z)=Ae^{ikz}\left(\lambda-y^2-\frac{iz}{k}\right),$$

$$E_y(y,z)=\frac{Ak}{k_0\varepsilon}e^{ikz}\left(\lambda-y^2-\frac{ikz+1}{k^2}\right),$$

$$E_z(y,z)=\frac{2iA}{k_0\varepsilon}e^{ikz}y, \tag{52}$$

where $k=k_0\sqrt{\varepsilon}$ (magnetic permeability is again the unity).

Further we will trace the development of the Poynting singularities with raising parameter λ. All the transformations of the singularities are summarized in the bifurcation diagram in Fig. 7. At $\lambda<0$ there is no critical points. First, complex singular point appears at $\lambda=0$ [Fig. 8(a)]. It is composed of four Poynting singularities, two vortices, and two saddles and looks like the obstacle preventing the energy density flow. The vertical line passing through the complex point divides the plane into two parts. In the right-(left-)hand side, the right-(left-)hand vortex becomes apparent. The simpler form of this complex critical point can be observed in Fig. 9(a). In this map of the magnetic field, the complex singular point presents the superposition of saddle (left-hand side of the figure) and stable node, namely, sink (right-hand side of the figure). Such a complex critical point is known to appear at the line $|G|=0$ separating saddles and nodes in the diagram in Fig. 4. However, stability matrix is now referred not to the Poynting vector, but to the complex function of magnetic field H_x.

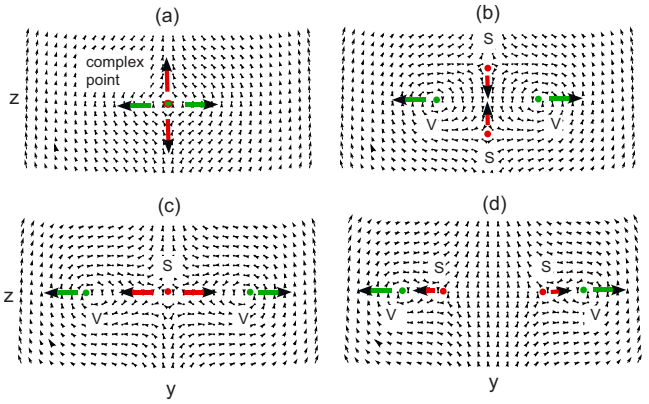

FIG. 8. (Color online) Poynting vector map (S_y is along the horizontal y axis and S_z is along the vertical z axis) for the bifurcation diagram in Fig. 7 at (a) $\lambda=0$, (b) $\lambda=0.2$, (c) $\lambda=0.4$, and (d) $\lambda=0.6$. Red and green arrows show the movement of singularities, vortices (V) and saddles (S), with increasing parameter λ.

Subsequent increase in parameter λ generates four Poynting singularities. As proved in Sec. V, the magnetic-field-induced singularities are always vortices (we consider the nonabsorbing media with real dielectric permittivity ε). The positions of these vortices are defined by the equation $H_x(y_0,0)=0$, i.e., $y_0=\pm\sqrt{\lambda}$. The signs concern the direction of the vortex rotation, + (−) is for the right- (left-) hand vortex. The square-root dependencies are shown in the bifurcation diagram in Fig. 7. Except the couple of vortices, the couple of polarization-induced saddles arises [Fig. 8(b)]. The saddles are placed in the z axis, and their positions can be calculated from the condition $\mathbf{S}(0,z_0)=\mathbf{0}$ as $z_0=\pm\sqrt{\lambda(1-\varepsilon k_0^2\lambda)}$. From the dependence $z_0(\lambda)$ we may note that λ is strictly confined by the values $0<\lambda<1/(\varepsilon k_0^2)$. The corresponding curves are marked dashed in Fig. 7. At first the saddles are disperse, but after $\lambda=1/(2\varepsilon k_0^2)$ they gather again. At $\lambda=1/(\varepsilon k_0^2)$ both saddles coincide [Fig. 8(c)]. As follows from Fig. 9(b), magnetic field singularities (saddle and sink) are simply dispersed. In this example of bifurcation behavior, the value $\lambda=1/(\varepsilon k_0^2)$ corresponds to the singularity of the electric field (in general, this is not the case), $\mathbf{E}(0,0)=\mathbf{0}$. In the Poynting map we call this situation as electric-field-induced singularity. The point (0,0) is the single point to result in the electric field singularity.

The further increase in the parameter λ generates the couple of polarization-induced saddles, which attract to the vortices for greater λ [Fig. 8(d)]. The positions of y-arranged polarization-induced singularities follow from $E_y(y_0,0)=0$; that is, $y_0=\pm\sqrt{\lambda-1/(\varepsilon k_0^2)}$.

Thus, we have considered the example of Poynting vector bifurcations. They are accompanied with the magnetic field and electric field bifurcations. The separate situation, typical for the Poynting vector behavior, is the presence of the polarization-induced singularities. They significantly change the bifurcation diagram of the system.

VII. CONCLUSION

This paper is intended for demonstrating the frame of the optical dynamic systems theory. We have revealed some basic features of the optical singularities, which are similar to what follows from the theory of dynamic systems. First of all, it is the proof of the equation for the image point (1). The image point moves in the natural three-dimensional space (such as phase space of a dynamic system). The point itself does not exist as realistic object; it is only one of the convenient descriptions of the field evolution. On the other hand, Poynting vector $\mathbf{S}$ (exactly, $\mathbf{S}/c^2$) is the momentum of the electromagnetic wave. That is why Eq. (1) results in the obvious statement that the velocity $\dot{\mathbf{r}}$ is proportional to the momentum. The realistic dielectric microparticle can be also affected by the averaged Poynting vector; however, the effect is not direct: the applied force is somehow expressed with $\mathbf{S}$.

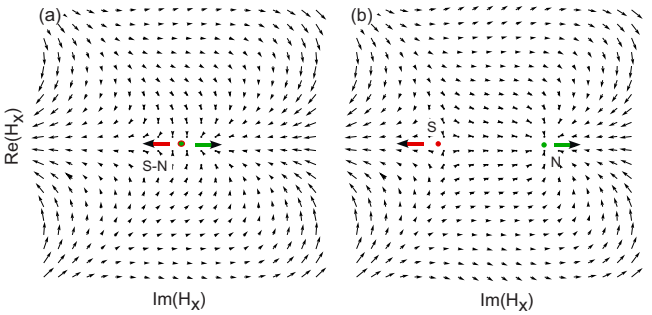

FIG. 9. (Color online) Vectorial map of complex function of magnetic field $H_x(y,z)$ at (a) $\lambda=0$ and (b) $\lambda=0.2$ (compare with bifurcation diagram in Fig. 7). The zeroes of magnetic field are the phase singularities: complex saddle-node point (S-N), saddle (S), or node (N).

We have obtained that the singularity of the Poynting vector can be caused by field vanishing or special polarization of the electromagnetic field. These singular points are called electric-(magnetic-)field-induced singularities and polarization-induced singularities, respectively. The positions of field-induced singular points coincide with that of phase singularities of the vector fields. All the situations (for linear and nonlinear field polarizations), in which polarization-induced singularities arise, have been analyzed in Sec. III. The critical points can be just isolated singular points or can form singular lines and surfaces. The behavior of the image point near the singular objects depends on the geometry of the singularity. In the case of the singular lines, the problem can be reduced to the two-dimensional one. The examples of the two-dimensional problems are considered in Secs. V and VI. The simplest case of singular surface can be studied in general: for the conservative dynamic systems the image point moves along the surface.

We have offered the calculation of the Poynting singularity type (vortex, focus, saddle, and node) of a two-dimensional system using the criterion based on the trace and determinant of the stability matrix. In this way, we have generally found the types of field-induced singularities without specifying certain field dependencies (Sec. V). Finally, we have considered the tangential bifurcation of the magnetic field and demonstrated some branching points for the bifurcation of the Poynting vector.

As future trends of the current work, we may suppose

investigating the fully three-dimensional field distributions, appearance of the limit cycles, and stochastic dynamic regimes. The theory developed can be applied for investigating optical singularities in the focal region, if the fields are presented in the certain form (e.g., in Debye approximation). Then polarization dependence of the local circulation [41] and super-resolution in high numerical aperture systems [42] can be analyzed.

[1] R. Merlin, Science **317**, 927 (2007).
[2] N. Fang, H. Lee, C. Sun, and X. Zhang, Science **308**, 534 (2005).
[3] I. I. Smolyaninov, Y.-J. Hung, and C. C. Davis, Science **315**, 1699 (2007).
[4] Z. Liu, H. Lee, Y. Xiong, C. Sun, and X. Zhang, Science **315**, 1686 (2007).
[5] G. Lerosey, J. de Rosny, A. Tourin, and M. Fink, Science **315**, 1120 (2007).
[6] V. P. Tychinsky, Phys. Usp. **51**, 1161 (2008).
[7] A. V. Volyar and T. A. Fadeeva, Opt. Spectrosc. **95**, 792 (2003); **96**, 96 (2004).
[8] A. L. Sokolov, Opt. Spectrosc. **104**, 134 (2008).
[9] L. E. Helseth, Opt. Commun. **281**, 1981 (2008).
[10] M. Perez-Molina, L. Carretero, P. Acebal, and S. Blaya, J. Opt. Soc. Am. A Opt. Image Sci. Vis. **25**, 2865 (2008).
[11] Special Issue on Rays and Beams, Proceedings of the IEEE, Vol. 62, 1974.
[12] F. I. Fedorov, *Theory of Gyrotropy* (Nauka i Tehnika, Minsk, 1976).
[13] F. I. Fedorov, *Optics of Anisotropic Media*, 2nd ed. (URSS, Moscow, 2004).
[14] J. F. Nye and M. V. Berry, Proc. R. Soc. London, Ser. A **336**, 165 (1974).
[15] I. Freund, Opt. Commun. **199**, 47 (2001).
[16] J. F. Nye and J. V. Hajnal, Proc. R. Soc. London, Ser. A **409**, 21 (1987).
[17] J. V. Hajnal, Proc. R. Soc. London **430**, 413 (1990).
[18] J. F. Nye, *Natural Focusing and Fine Structure of Light: Caustics and Wave Dislocations* (Institute of Physics, Bristol, 1999).
[19] M. V. Berry and M. R. Dennis, Proc. R. Soc. London **456**, 2059 (2000).
[20] I. Freund, M. S. Soskin, and A. I. Mokhun, Opt. Commun. **208**, 223 (2002).
[21] I. Freund, Opt. Commun. **242**, 65 (2004).
[22] I. Freund, Opt. Commun. **196**, 63 (2001).
[23] I. Freund, Opt. Commun. **272**, 293 (2007).
[24] M. V. Berry and M. R. Dennis, Proc. R. Soc. London **459**, 1261 (2003).
[25] M. V. Berry, Proc. R. Soc. London **461**, 2071 (2005).
[26] G. N. Borzdov, Phys. Rev. E **61**, 4462 (2000).
[27] A. Ya. Bekshaev and M. S. Soskin, Opt. Commun. **271**, 332 (2007).
[28] M. A. H. Bateman, *The Mathematical Analysis of Electrical and Optical Wave-Motion on the Basis of Maxwell's Equations* (Dover, New York, 1955).
[29] I. Bialynicki-Birula and Z. Bialynicki-Birula, Phys. Rev. A **67**, 062114 (2003).
[30] M. V. Berry, J. Opt. A, Pure Appl. Opt. **6**, S175 (2004).
[31] A. A. Andronov, A. A. Vitt, and S. E. Khaikin, *Theory of Oscillators* (Dover, New York, 1987).
[32] J. Bajer and R. Horák, Phys. Rev. E **54**, 3052 (1996).
[33] A. Lakhtakia, *Beltrami Fields in Chiral Media* (World Scientific, Singapore, 1994).
[34] L. M. Barkovsky and A. N. Furs, *Operator Methods for Describing Optical Fields in Complex Media* (Belaruskaya Navuka, Minsk, 2003).
[35] A. V. Novitsky and D. V. Novitsky, J. Opt. Soc. Am. A **24**, 2844 (2007).
[36] A. V. Novitsky and D. V. Novitsky, Opt. Commun. **281**, 2727 (2008).
[37] A. V. Novitsky, L. M. Barkovsky, J. Opt. A, Pure Appl. Opt. **10**, 075006 (2008).
[38] V. I. Kuvshinov and A. V. Kuzmin, Phys. Lett. A **296**, 82 (2002).
[39] R. Z. Sagdeev, D. A. Usikov, and G. M. Zaslavsky, *Nonlinear Physics: From the Pendulum to Turbulence and Chaos* (Harwood, New York, 1988).
[40] B. Z. Katsenelenbaum, J. Commun. Technol. Electron. **42**, 119 (1997).
[41] L. E. Helseth, Opt. Commun. **229**, 85 (2004).
[42] S. F. Pereira and A. S. van de Nes, Opt. Commun. **234**, 119 (2004).